

1 *Type of the Paper (Article)*

# 2 **Polymeric nanocomposites membranes with high** 3 **permittivity based on PVA - ZnO nanoparticles for** 4 **potential applications in flexible electronics**

5 **Roberto Ambrosio**<sup>1\*</sup>, **Amanda Carrillo**<sup>2</sup>, **Maria de la Luz Mota**<sup>2</sup>, **Karla de la Torre**<sup>2</sup>,  
6 **Richard Torrealba**<sup>1</sup>, **Mario Moreno**<sup>3</sup>, **Hector Vazquez**<sup>4</sup>, **Javier Flores**<sup>1</sup> and **Israel Vivaldo**<sup>1</sup>

7

8 <sup>1</sup> Electronic Department, Meritorious Autonomous University of Puebla, 72590, Pue., Mexico,

9 [roberto.ambrosio@correo.buap.mx](mailto:roberto.ambrosio@correo.buap.mx) (R.A), [richard.torrealba@correo.buap.mx](mailto:richard.torrealba@correo.buap.mx) (R.T),

10 [xavier\\_snk@hotmail.com](mailto:xavier_snk@hotmail.com) (J.F), [israelvivac@gmail.com](mailto:israelvivac@gmail.com) (I.V)

11 <sup>2</sup> Electrical Department, Ciudad Juarez Autonomous University 32310, Chih. Mexico,

12 [amanda.carrillo@uacj.mx](mailto:amanda.carrillo@uacj.mx) (A.C), [maria.mota@uacj.mx](mailto:maria.mota@uacj.mx) (M.M)

13 <sup>3</sup> Electronic Department, National Institute for Astrophysics Optics and Electronics, 72000, Pue., Mexico,  
14 [mmoreno@inaoep.mx](mailto:mmoreno@inaoep.mx)

15 <sup>4</sup> Electronic Instrumentation and Atmospheric Sciences School, University of Veracruz, Xalapa, México,  
16 [hvazquez@uv.mx](mailto:h vazquez@uv.mx)

17 \* Correspondence: [roberto.ambrosio@correo.buap.mx](mailto:roberto.ambrosio@correo.buap.mx); Tel.: +52 (222) 229 55 00

18

19 **Abstract:** In this study is reported the optical, structural and dielectric properties of Poly (vinyl  
20 alcohol) thin films membranes with embedded ZnO nanoparticles (PVA/ZnO) obtained by solution  
21 casting method at low temperature of deposition. Fourier Transform Infrared spectra showed the  
22 characteristics peaks, which correspond to O-H and Zn-O bonds present in the hybrid material. The  
23 X-ray diffraction patterns indicated the presence of ZnO structure into the films. The composite  
24 material showed low absorbance and a wide band gap energy from 5.6 to 5.9 eV. The surface  
25 morphology for the thin films of PVA/ZnO was studied by Atomic Force Microscopy and Scanning  
26 Electron Microscopy. The dielectric properties of the nanocomposites were measured from low to  
27 high frequencies, the results showed a high dielectric constant ( $\epsilon$ ) in the order of  $10^4$  at low frequency  
28 and values from  $\epsilon \approx 2000$  to 100 in the range of 1KHz-1MHz respectively, the properties of PVA/ZnO  
29 such as the high permittivity and the low temperature of processing make it a suitable material for  
30 potential applications in the development of flexible electronic devices.

31 **Keywords:** solution process; thin films; composite material; dielectric constant

32

## 33 **1. Introduction**

34 Composite materials based on a polymeric matrix with embedded metal nanoparticles have gain  
35 attention due to their properties such as electrical, mechanical, optical and chemical properties that  
36 can be used in the development of biomedical devices, solar cells, sensors, capacitors among others  
37 [1] [2]. A hybrid material consists of soluble polymers with inorganic component with excellent  
38 mechanical, optoelectronics and dielectric properties due to the combination of the organic and  
39 inorganic components, and it can be deposited as a thin film in different substrates. Therefore, the  
40 number of contributions in the development of hybrid composites based on polymers and  
41 nanoparticles with high permittivity, low cost, and easily tunable properties, have become a hot topic  
42 in the research of materials [3]. Recently, some works have been reported the integration of thin films  
43 based on polymeric materials such as Polyvinyl alcohol (PVA) as a gate dielectrics for the  
44 development of organic Thin Film Transistors (TFT), due to the high dielectric constant which  
45 enhances the gate capacitance, with the advantages of solution processable material, at low cost, non-

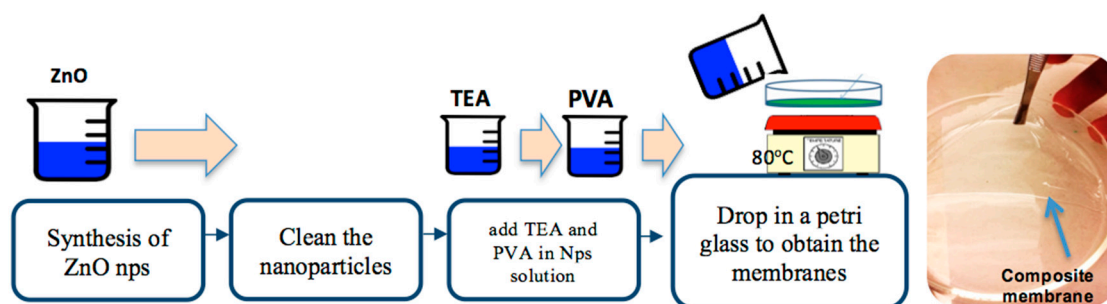
46 toxic, with flexible hydrophilic network and low temperature of deposition [4] [5]. PVA is a poor  
47 electric conductor, water soluble, it has carbon chain backbone with OH groups and it is eco-friendly,  
48 and its physical properties may be adapted to a specific requirement in conjunction with inorganic  
49 materials [6]. On the other hand, nanoparticles of Zinc oxide (ZnO Nps) have been used in memory  
50 devices, gas sensors, thin film devices, and flexible electronic devices [7], [8]. Furthermore, the  
51 utilization of ZnO as semiconductive filler to prepare high dielectric constant polymer composites  
52 has been reported [9]. Related to hybrid materials, few studies have investigated the dielectric  
53 properties of PVA with embedded ZnO nanoparticles into the polymeric matrix. J.J. Mathen et al.  
54 synthesized membranes of PVA/ZnO for developed of an UV-A sensor on an ITO substrate showed  
55 the interfacial interaction between the filler and the matrix resulting in a large improvement in the  
56 dielectric, optical and mechanical properties [1]. P. I. Devi et al. studied the dielectric properties of  
57 a hybrid composite based on Polyvinylidene fluoride PVDF-ZnO for microwave frequencies, it  
58 showed a decrease in dielectric constant and dielectric loss with the frequency, and the ZnO  
59 composition has a great influence on the trend and magnitude of dielectric properties [10].  
60 Sugumaran et al. obtained a hybrid poly (vinyl alcohol)-indium zinc oxide (PVA-InZnO) thin films  
61 by a simple dip coating method with dielectric constant values around 6 to 20 [11]. Recently, a  
62 nanocomposite polymer films based on PVA and TiO<sub>2</sub> nanoparticles have been reported with relative  
63 high permittivity [12]. Therefore there is an interest in order to obtain a composite material with a  
64 high dielectric constant which to meet the requirements for flexible electronics such as low  
65 temperature of deposition, stability, flexibility and low cost. In this work, is reported the synthesis  
66 and characterization of a Poly(Vinyl Alcohol) thin films with embedded ZnO nanoparticles (ZnO  
67 Nps) by solution casting method, taking the advantage that the electrical and optical properties can  
68 be tuned by adding ZnO nanoparticles into a polymeric matrix. The nanocomposites have been  
69 characterized using Fourier Transform Infrared spectroscopy (FTIR), Scanning Electron Microscopy  
70 (SEM), UV-vis spectroscopy to determine band gap, and Atomic Force Microscopy (AFM) for surface  
71 roughness of the membranes. The dielectric properties of PVA-ZnO nanocomposites were measured  
72 from low to high frequencies. The results show high dielectric constant ( $\epsilon$ ) at low frequencies, even  
73 at high frequencies  $\epsilon$  is higher than other related composites materials, thus the hybrid PVA-ZnO  
74 Nps make it a suitable for potential applications in electronic devices.

## 75 2. Materials and Methods

### 76 2.1 Materials

77 For the synthesis was used Polyvinyl Alcohol (PVA) from sigma aldrich with an average  
78 molecular weight  $M_w=130,000$  and 99% hydrolyzed to obtain the membranes. A solution of PVA was  
79 prepared using 2.5g powder in 50 ml of distilled water and stirred at 90°C in order to obtain a  
80 homogenous solution. For ZnO Nps, Sodium Dodecyl Sulfate (SDS), Zinc chloride (ZnCl<sub>2</sub>), Acid  
81 Citric (C<sub>6</sub>H<sub>8</sub>O<sub>7</sub>), Potassium Hydroxide (KOH) and Ammonia (HN<sub>4</sub>) were used to form ZnO  
82 nanoparticles. The general process is depicted in Figure. 1.

83



84

85

Figure 1. General sequence of synthesis of PVA/ZnO membranes

## 86 2.1.2 Preparation of PVA/ZnO membranes

87 The membranes as thin films were prepared by solution casting method, following the next  
 88 steps: firstly, the solution of ZnO nanoparticles was cleaned with distilled water. The next step was  
 89 to add 0.3 ml of trietanolamylene (TEA) (1M) in 3 ml of nanoparticles solution; then 19.2 ml of PVA  
 90 that was previously prepared was added. Finally, the solution was deposited on glass petri dishes  
 91 and it was heating at 80°C for 40 minutes to obtain the membranes. The quantities for the precursors  
 92 in the synthesis of ZnO nanoparticles are listed and labeled in Table 1.  
 93

94 **Table 1.** Details of the solutions to synthesize ZnO nanoparticles

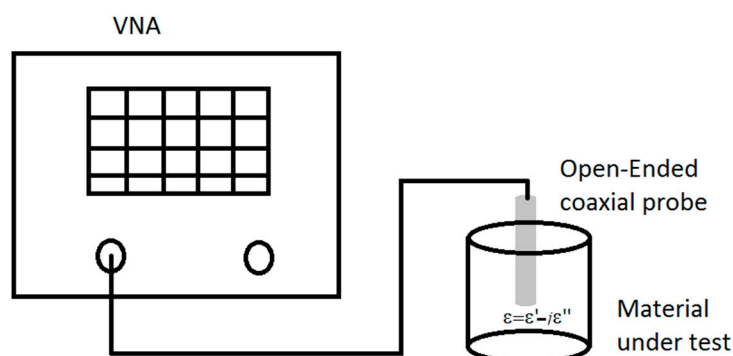
95 Sample Name	96 SDS	ZnCl <sub>2</sub>	C <sub>6</sub> H <sub>8</sub> O <sub>7</sub>	97 Solution
Z1	5 ml	1 ml	1 ml	NH <sub>4</sub>
Y1	5 ml	1 ml	1 ml	KOH
Z4	5 ml	2.5 ml	1.2 ml	NH <sub>4</sub>
Y4	5 ml	2.5 ml	1.2 ml	KOH

100

## 101 2.2. Characterization

102 The ZnO Nps were chemical, optical and structural characterized using the methods of Fourier  
 103 Transform Infrared Spectroscopy (FTIR), Ultra Violet-Visible spectra measured by UV- Vis, model  
 104 6850 Jenway spectrometer, and morphology by Scanning Electron Microscopy (SEM) as well as  
 105 Energy Dispersive Spectroscopy (EDS) was included for the composition analysis of the thin films  
 106 and the structure was determined by X-ray diffraction (XRD 20 to 80  $\theta$ ).

107 For the dielectric properties of the material, firstly, the solutions of PVA/ZnO Nps were measured  
 108 using the open-ended coaxial probe technique [13]. This technique was implemented using a  
 109 Keysight Vector Network Analyzer and the open-ended coaxial performance probe (Keysight  
 110 N1501A Dielectric Probe Kit). The Figure 2 shows the setup of the open-ended coaxial probe  
 111 technique. The measurements were performed in a frequency range from 0.5GHz to 20GHz and  
 112 the system was calibrated using air and distilled water.



113

114 **Figure 2.** Setup of the open-ended coaxial probe technique for dielectric measurements in the solution  
 115 of PVA/ZnO Nps

116 Using the equation (1) where  $\epsilon'$  is the dielectric constant and  $\epsilon''$  is the loss factor is possible to  
117 obtain the conductivity and the tangential loss ( $\tan\delta$ ) which is determined by the equations (2) and  
118 (3)

$$\epsilon = \epsilon' - j\epsilon'', \quad (1)$$

$$\sigma = 2\pi f \epsilon'' \epsilon_0, \quad (2)$$

$$\tan\delta = \frac{\epsilon''}{\epsilon'}, \quad (3)$$

119 where  $f$  is the frequency in Hz and  $\epsilon_0$  is the permittivity in the vacuum.

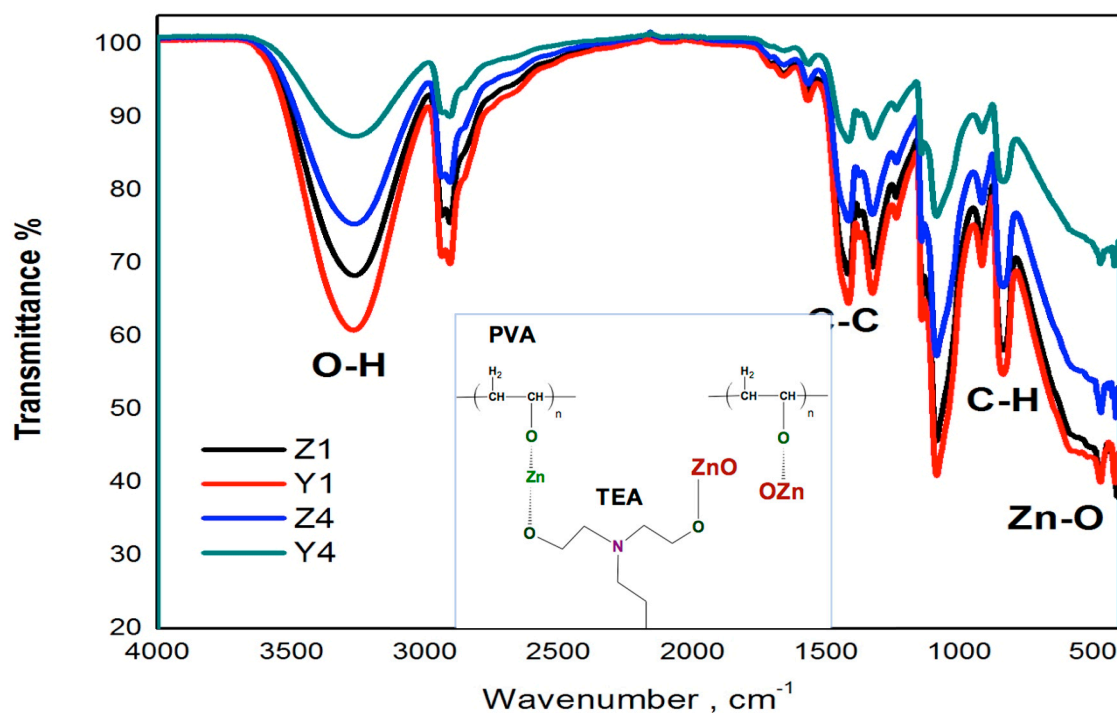
120 Later a Metal-Insulator-Metal structure was fabricated on the membranes using aluminum as top and  
121 bottom electrodes. Aluminum circular contacts with a diameter of 2000  $\mu\text{m}$  and a thickness of 300nm  
122 were deposited by e-beam evaporation through a shadow mask. The dielectric constant of the  
123 PVA/ZnO membranes was carried out using the MIM structure and LCR impedance analyzer (HIOKI  
124 LCR model 3536) at room temperature and a constant voltage of 1 Vrms in the frequency range from  
125 500 Hz to 1 MHz.  
126

### 127 3. Results and discussion

#### 128 3.1 FTIR analysis

129 In order to determine the chemical bonds in the PVA and ZnO nanoparticles, the FTIR spectrum  
130 was measured in the membranes, which is showed in fig. 3. The peak at 3267  $\text{cm}^{-1}$  is due to OH groups  
131 in the polymer backbone, the peaks at 2906  $\text{cm}^{-1}$  and 918  $\text{cm}^{-1}$  are due to CH<sub>2</sub> asymmetric and  
132 symmetric stretching, respectively. The peak observed around 1420  $\text{cm}^{-1}$  is due to C-C stretching  
133 which is in accordance to reference [14]. Furthermore, the band observed at 420-417  $\text{cm}^{-1}$  is due to  
134 Zn-O stretching, this suggest the presence of ZnO into the membranes.

135 The interaction of PVA bonds with the addition of ZnO nanoparticles is attributed by the  
136 intermolecular interaction between OH groups by PVA and the surface of the nanoparticles [15].  
137 The hydroxyl groups of PVA have a strong tendency to form a charge transfer complex with ZnO  
138 nanoparticles through chelation [16]. The addition of TEA in the solution allows the complete  
139 interaction between the nanoparticles and the polymer and also provides a dispersion of the  
140 nanoparticles avoiding agglomerates. The bands of PVA are more or less pronounced depending if  
141 KOH or NH<sub>4</sub> is employed in the synthesis, and also it depends of nanoparticles concentration into  
142 the polymer (PVA) matrix, thus the intensity of the OH bonds are decreasing as the amount of ZnO  
143 increases. Hydroxyls groups are the most representatives to analyze the chemical changes due to  
144 evident reduction intermolecular interactions to provide the composites formation. The chemical  
145 reaction of PVA with ZnO and its precursors is shown in the inset of Figure. 3. PVA can be chemically  
146 or thermally cross-linked at their hydroxyl groups generate water as a by-product [17].  
147



148

149

150

**Figure 3.** FTIR spectra of PVA matrix with ZnO nanoparticles, the inset shows the reaction of PVA and ZnO.

151

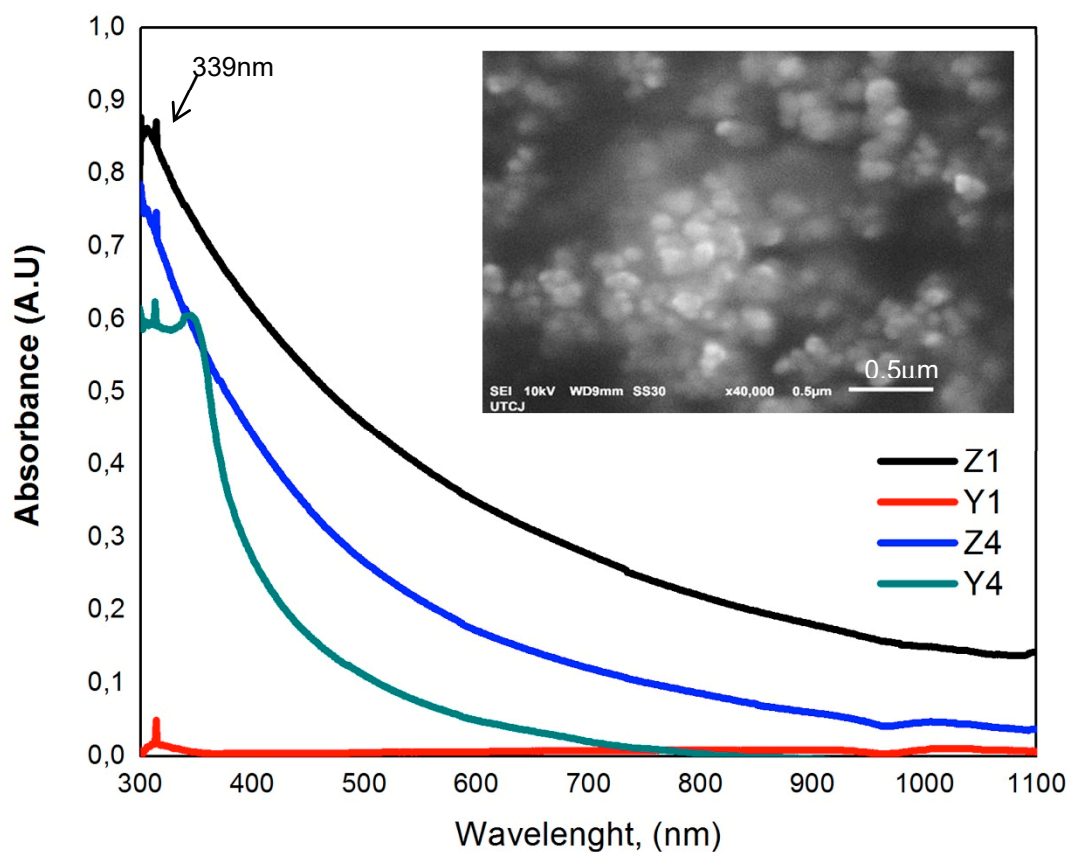
### 152 3.1. Absorbance characteristics and optical band gap

153 The UV-Vis absorbance spectra for the ZnO Nps is shown in fig. 4, in the samples there is a peak  
 154 at 339 nm, close to 385nm which corresponds to the bulk ZnO [18], it is identified due to the addition  
 155 of ZnO nanoparticles, consequently, this is an indication of the interaction between PVA and ZnO,  
 156 the inset of Figure. 4 is a SEM image for the ZnO Nps corroborating the aspheric morphology and  
 157 the completely formation of the nanoparticles. Prior to embedded the ZnO into the PVA, the Tauc's  
 158 method was used to calculate the ZnO band gap ( $E_g$ ), obtaining a mean value of 3.9 eV, that is a high  
 159 value for ZnO obtained from a chemical method. Figure 5a shows the UV-Vis absorbance spectra in  
 160 the region from 200 to 1100 nm for PVA/ZnO Nps membranes. From the spectra is possible to observe  
 161 that the absorption for all films decreased with increasing wavelength, while for the samples Y4 and  
 162 Z4, the absorption increased with increasing ZnO content. This is in agreement with the reported by  
 163 reference [16], where the absorption is proportional to the number of absorbing molecules and it  
 164 increases with increasing weight % of ZnO.

165 In Figure 5b is plotted the band gap ( $E_g$ ) of the PVA/ZnO membranes, The  $E_g$  values are in the range  
 166 from 5.6 to 5.9 eV, the samples prepared from the  $\text{NH}_4$  (sample Z4) showed the high value due to the  
 167 agglomeration of nanoparticles, however the  $E_g$  values are very closed to each other, which is and  
 168 indicative that there are no significantly changes in the structure of the hybrid material and a good  
 169 dispersion of the ZnO Nps is presented into the polymeric matrix.

170

171



172

173

174

**Figure 4.** UV-Vis absorbance spectra of ZnO nanoparticles synthesized at different contents, the inset shows a SEM image for one of the ZnO nanoparticles agglomeration.

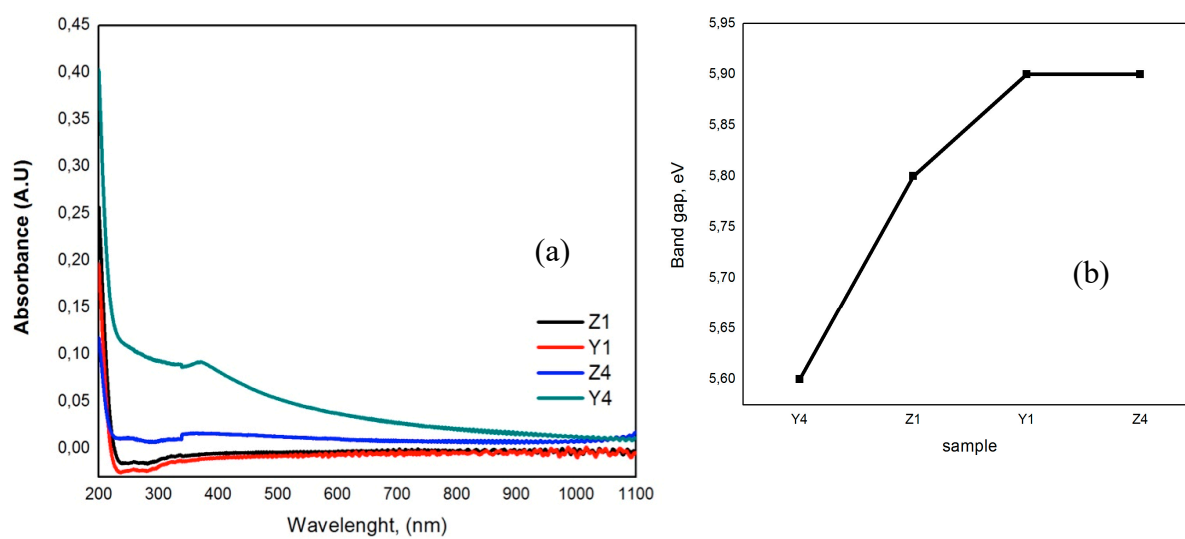
175

176

177

178

179



180

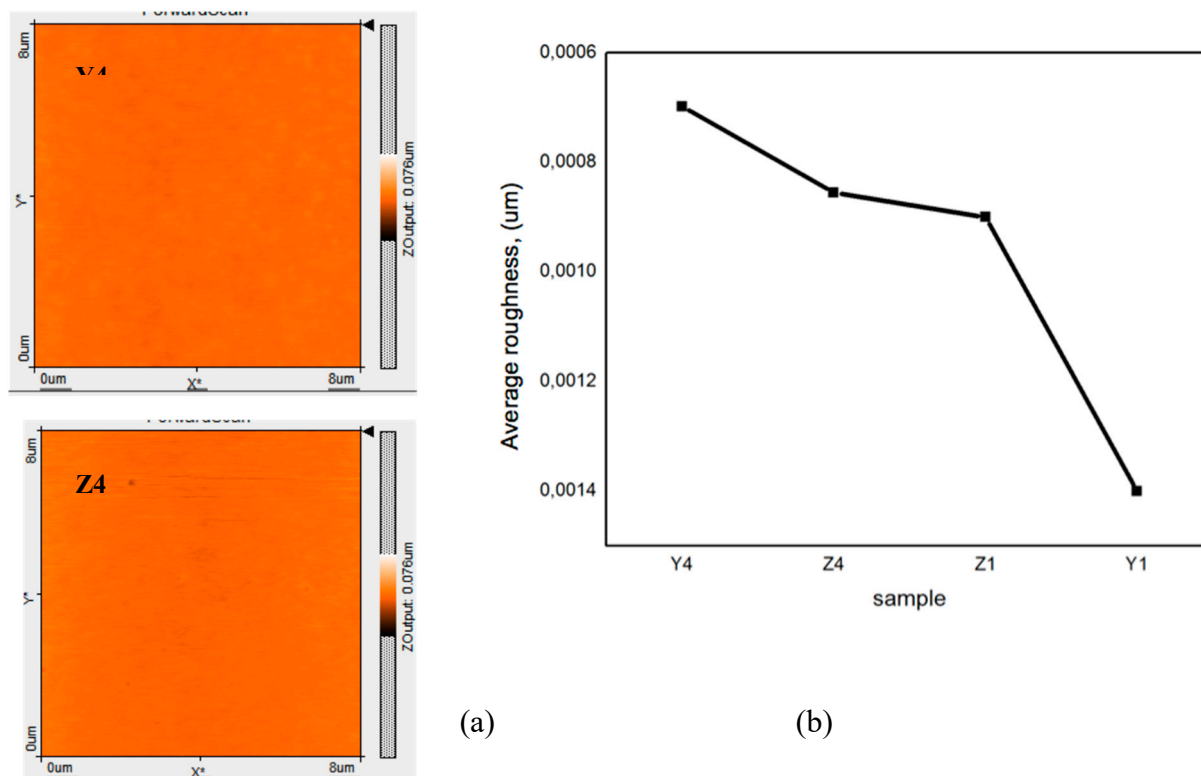
181

**Figure 5.** (a) Absorbance spectra of PVA-ZnO Nps; (b) Band gap obtained for the samples.

182

### 183 3.3 Surface morphology

184 In Figure 6a is shown the surface morphology for two samples with different concentration of  
 185 ZnO nanoparticles into the membranes. In the Figure. 6b is showed the variation of the average  
 186 roughness of the film as a function of the precursors  $\text{NH}_4$  or KOH for ZnO Nps. The membranes  
 187 prepared with low ZnO nanoparticles concentration showed low roughness (samples Z1 and Y1), is  
 188 possible to observe that all samples have a homogeneous topography and low roughness.  
 189  
 190



191  
 192

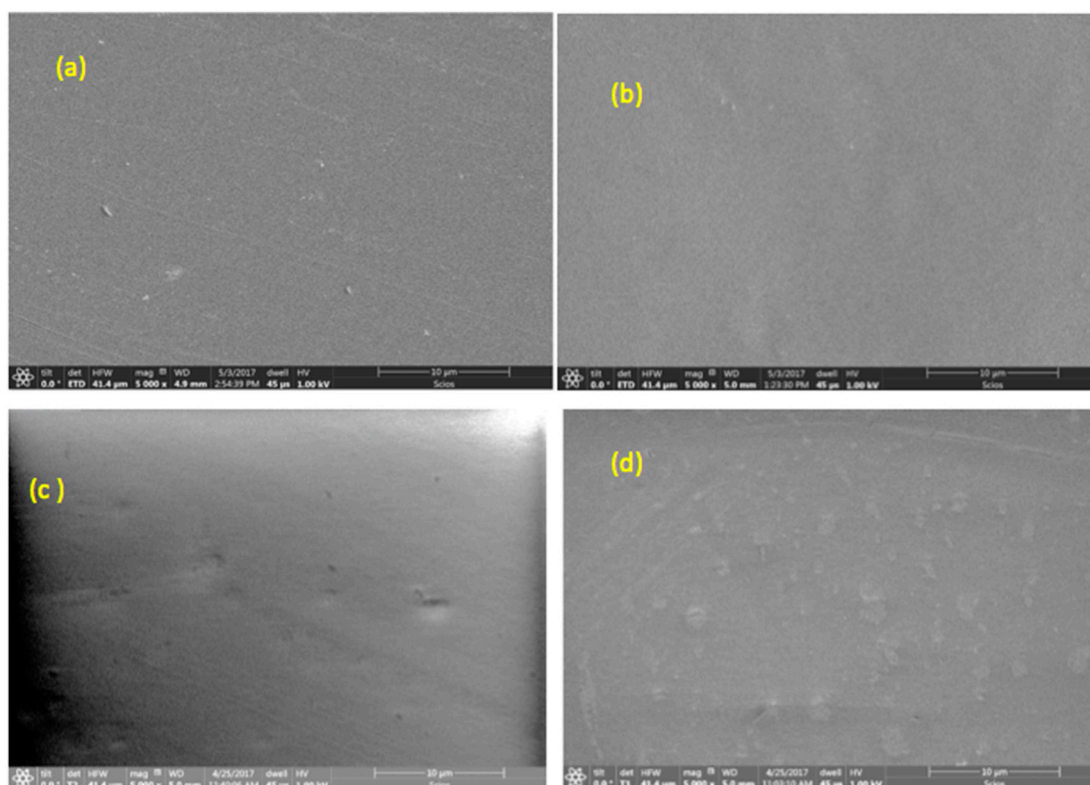
193 **Figure 6.** (a) AFM topography for samples Z4 and Y4; (b) Average roughness for PVA-ZnO  
 194 membranes.

195 The Scanning electron micrographs of PVA/ZnO Nps membranes are shown in Figure. 7 (a-d).  
 196 SEM images showed ZnO nanoparticles distribution in the polymer membrane. The formation of  
 197 agglomerates is observed when the ZnO concentration increases for samples Y4 and Z4, however  
 198 homogeneous agglomeration distribution is obtained in all samples. This distribution is attributed to  
 199 the wet chemistry process used to obtain ZnO nanoparticles in solution where the ZnO Nps are  
 200 compatible with the process to obtain the polymer. The ZnO nanoparticles synthesized by sol gel-  
 201 method showed a size of 100 nm from samples obtained with the use of KOH or  $\text{NH}_4$  precursors.  
 202

### 203 3.4 Structural analysis

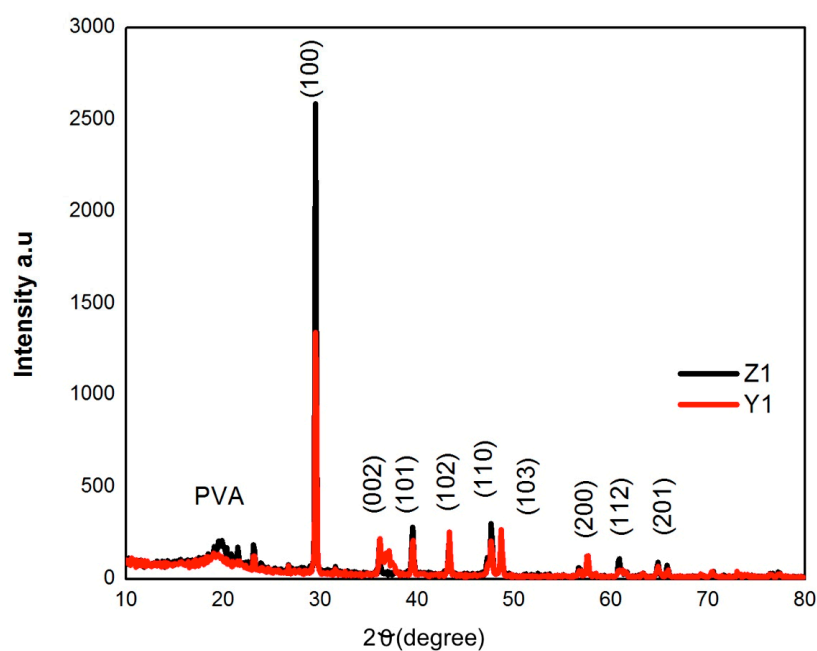
204 The X-ray diffraction pattern (XRD) for PVA/ZnO membranes is showed in Figure 8. The broad  
 205 diffraction peak located at  $2\theta = 21.53^\circ$  is due to amorphous PVA [11]. Peaks located at  $2\theta = 29.5^\circ$ ,  $36.1^\circ$ ,  
 206  $39.5^\circ$ ,  $43.2^\circ$ ,  $47.6^\circ$  and  $48.6^\circ$  corresponding to (100) (100) (102) (110) and (103) respectively, the  
 207 reflection plane of ZnO, showing the presence and hexagonal structure of the nanoparticles, and c-  
 208 axis orientation, in addition to well-defined diffraction peaks indicating complete crystal formation  
 209 [1] [19]. The values of interplanar spacing (d), the average of lattice parameters and the unit cell (u)

210 in the membranes were obtained by Bragg law, resulting as follows  $d = (3.0201 \text{ \AA}, 3.0206 \text{ \AA})$  and  $u = (76$   
 211 and  $69 \text{ nm})$  respectively.  
 212



213  
 214

**Figure 7.** SEM images for PVA-ZnO membranes: a) Z1, b) Y1, c) Z4, d) Y4.



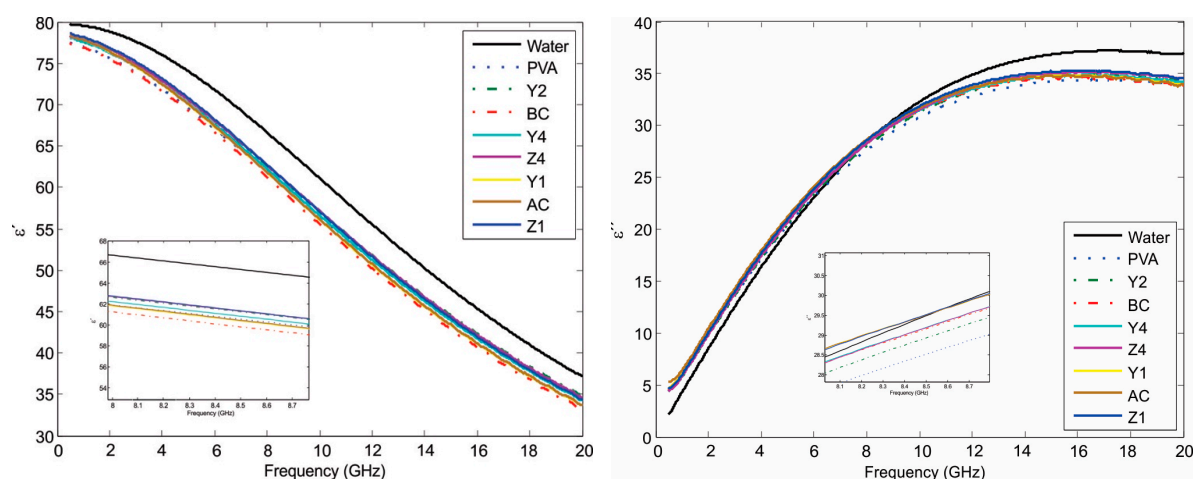
215  
 216  
 217

**Figure 8.** XRD pattern of PVA/ZnO Nps membranes

### 218 3.4 Dielectric properties

219 For the analysis of dielectric properties, firstly the solution of PVA/ ZnO Nps was analyzed with  
 220 the technique that was described in the experimental section, for this study distilled water was used  
 221 as dielectric reference and also for the calibration, the measurements were performed in the range  
 222 from 0.5-20 GHz at room temperature. The relative permittivity of water is  $\epsilon' \approx 80$ , as is shown in the  
 223 Figure 9(a), therefore the dielectric constant ( $\epsilon'$ ) values of PVA/ ZnO Nps are closer to the permittivity  
 224 of water at 500MHz, this is due to the water component in the PVA solution. In addition, Figure 9(a)  
 225 and (b) show the variation in the dielectric constant ( $\epsilon'$ ), and loss factor ( $\epsilon''$ ) with frequency for  
 226 different content of ZnO Nps, in the insets of figures is possible to observe the variations, the dielectric  
 227 constant for the solution of the PVA with ZnO nanoparticles which decreases as frequency increases,  
 228 this is in accordance with the reported by Yeow et al, and could be explained due to the dipoles which  
 229 are not able to follow the variation field at higher frequencies [19]. At relative low frequencies in the  
 230 range for microwave applications the solution for the membranes showed a high dielectric constant,  
 231 and it is related to electrode polarization of the polymer [20].

232



233

234 **Figure 9.** (a) The dielectric constant ( $\epsilon'$ ); and (b) loss factor ( $\epsilon''$ ) as a function of the frequency for  
 235 various ZnO nanoparticles content in PVA solution.

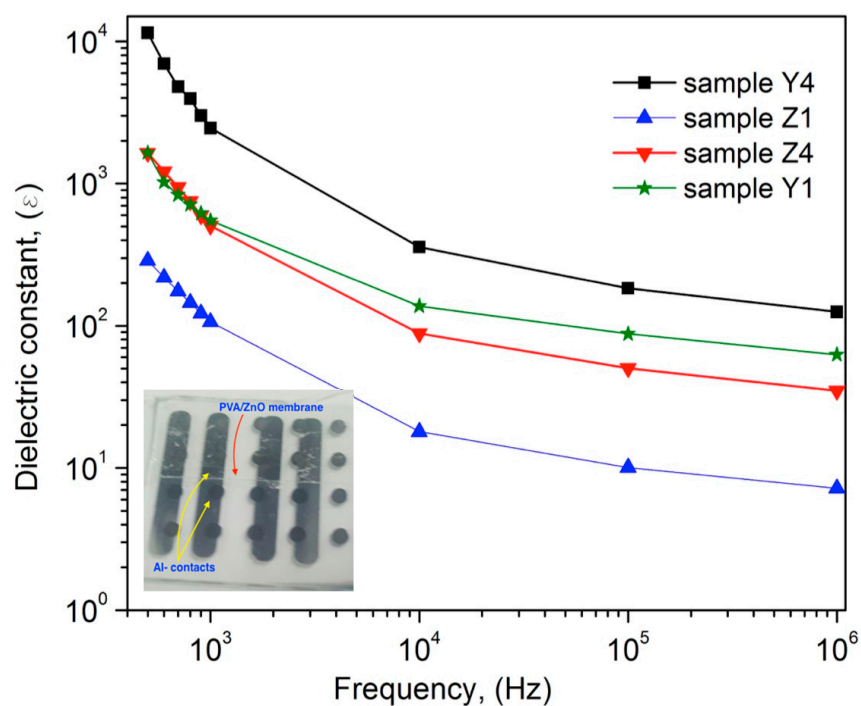
236 Figure 10 shows the dielectric constant as a function of frequency for the PVA membranes with  
 237 different content of ZnO Nps, the measured capacitance with the LCR equipment was used to  
 238 calculate the dielectric constant in the films, the inset in the figure 10 shows one of the samples used  
 239 for the characterization. From the figure 10 is possible to observe the influence at low frequency on  
 240 the dielectric constant, which is high for all samples, and the value decrease with frequency increases,  
 241 this trend is similar to the reported by other authors, however the maximum value of  $\epsilon' = 11468$   
 242 obtained for the sample Y4 at 500Hz is higher than the reported by other works, in table 2 is showed  
 243 a comparison with materials, methods and permittivity values [5]. At lower frequencies, all the free  
 244 dipolar functional groups present in PVA polymeric chain can align themselves resulting higher  
 245 permittivity values [20]. For frequencies up to 1KHz, the bigger dipolar groups find difficulty to  
 246 orient at the same pace as the alternating field, so the contributions of this dipolar group decrease  
 247 and also the permittivity [16]. The permittivity in ZnO nanoparticles also decreases when increases  
 248 frequency of the applied field, this is due to ZnO is a polar ceramic material with relatively high  
 249 permittivity therefore, the  $\epsilon'$  values of the nanocomposites are also found higher [21]. In addition, the  
 250 ZnO Nps embedded in the PVA matrix enhances the dielectric permittivity of the composite, because  
 251 ZnO exhibits a strong ionic polarization due to  $Zn^{2+}$  and  $O^{2-}$  ions and has a high value of static  
 252 permittivity [22]. Therefore, the samples Z4 and Y4 presented the higher value, further, the  
 253 increasing of  $\epsilon'$  values in the composites obtained at low frequencies can be attributed to the interfacial

254 polarization, which exhibits due to the difference in the permittivity values of the ZnO and the PVA  
 255 matrix.

256 **Table 2.** Comparison of permittivity values with related works of Polymer matrix/ZnO

Material	Deposition method and Temperature	Permittivity ( $\epsilon$ ) Frequency	Reference
PVA/ZnO membranes	Solution casting/ 50°C	17,8 at 100 Hz	[1]
PVDF/xGnPs	Solution mixing process	2,080 at 10 <sup>3</sup> Hz (4.1 vol%)	[2]
PVDF/ZnO composites	combination of solution blend, sequential precipitation, and hot-press processes/ °60C	100 at 500HZ	[9]
PVA/ZnO nanocomposites	Solution casting/ 40 °C	500 at 10 <sup>2</sup> Hz 10 <sup>2</sup> at 10 <sup>6</sup> Hz	[14]
PVDF/ZnO nanowires clusters	Microemulsion / 80°C	113 at 10 <sup>2</sup> Hz	[23]
Ag/TiO <sub>2</sub> / polytetrafluoroethylene (PTFE)	solution blended process 80°C	100AT 10 <sup>3</sup> Hz	[26]
PVA/ZnO	Solution casting method 80°C	≈10 <sup>4</sup> at 500Hz	This work

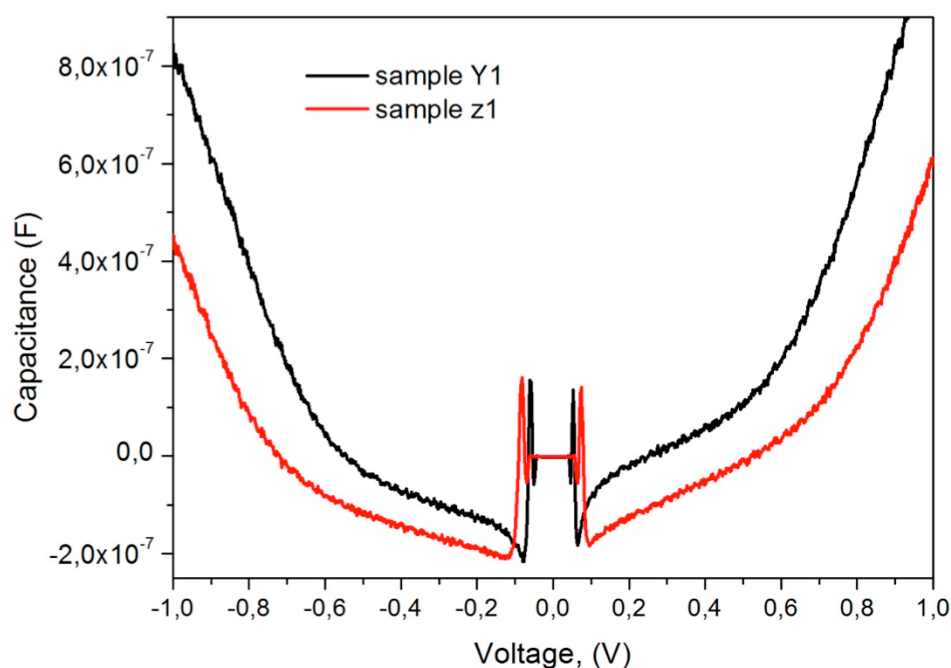
257



258

259 **Figure 10.** Variation of dielectric constant with frequency for the membranes of PVA with different  
 260 content of ZnO Nps. The inset is a picture of one the fabricated capacitors over glass substrates.

261 Capacitance-Voltage (C-V) curves were measured as an additional characterization in order  
262 to corroborate the high dielectric constant of the composites, the data were obtained with  
263 4200A Keithley semiconductor parameter analyzer at 1 KHz with a voltage sweeping from  
264 -1V to 1 V, the Figure 11 shows the C-V plot for the samples Y1 and Z1 identifying the three  
265 regions: accumulation, depletion and inversion, from accumulation region the dielectric  
266 constant was extracted with a value  $\epsilon \sim 10^9$  which is close to the obtained with the  
267 impedance analyzer and the value reported here is one of the highest using ZnO  
268 semiconductor nanoparticle for the composite.



269

270 **Figure. 11.** C-V measurements for the samples Y1 and Z1 (PVA/ZnO)

271

272 The introduction of conductive or semiconductive inorganic particles into the polymer  
273 matrix has resulted in dielectric composites with an effective permittivity that is much  
274 higher than that of the matrix. Relative permittivity ( $\epsilon_r$ ) values of up to  $10^5$  have been  
275 reported in some composite systems [24]. Large dielectric constant can be achieved in  
276 composites; the physical reason for the critical behavior of the dielectric constant near  
277 percolation is the existence of microcapacitor networks. Each microcapacitor is formed by  
278 the neighboring conductive filler particles and a very thin layer of dielectric in between and  
279 contributes an abnormally large capacitance mainly due to the introduction of nanofiller  
280 [25]. Further studies are necessary to investigate the effect of the filler shape on dielectric  
281 constant and breakdown strength of the PVA/ZnO composites, however the higher  
282 dielectric values in these membranes are very attractive for applications as an insulator in  
283 TFT for flexible electronics due to the compatible process for the semiconductor materials  
284 and also its low temperature of processing. For future work, we are taking in account to  
285 fabricate electronic devices such as thin film transistor to obtain some basic digital gates  
286 using a complete process with the integration of the dielectric material and semiconducting  
287 materials obtained in solution process in flexible substrate .

#### 288 4. Conclusions

289 Composites polymers based in membranes of PVA/ZnO NPs were prepared by solution casting  
290 process. The thin films were studied by the structural, optical and dielectric characterization. The

291 FTIR analysis demonstrated a good interaction between PVA matrix and the ZnO Nps, in samples  
292 with more ZnO Nps the O-H groups decrease, while in the samples prepared using NH<sub>4</sub> as the  
293 precursor a reduction in the O-H groups is observed. The UV-vis analysis showed that the addition  
294 of ZnO nanoparticles affect the absorbance close to the UV region and the maximum band gap is  
295 5.9eV for the sample with the higher ZnO content. The XRD analysis showed that the crystal structure  
296 of ZnO is presented in the PVA matrix. The surface morphology of the PVA/ZnO obtained by AFM  
297 showed a smoother surface with average roughness close to 1nm, and the SEM images presented an  
298 uniform dispersion of ZnO nanoparticles in the PVA. In general structural and chemical analysis  
299 confirmed that the ZnO nanoparticles were embedded into the PVA matrix. The dielectric properties  
300 of PVA depend on frequency and also in the ZnO content, thus in this work was obtained a hybrid  
301 material using semiconductive nanoparticles with the highest dielectric constant due to the  
302 interaction of nanoparticles, therefore these nanocomposites thin films are very promising material  
303 for applications in the develop of transistors for flexible electronics.

304 **Author Contributions:** Dr. R. Ambrosio, Dra. A. Carrillo and Dr. M. Mota prepared and designed the  
305 experiments. Karla de la Torre performed the experiments. R. TorreAlba determined the dielectric properties at  
306 High Frequencies. J. Flores and H. Vazquez analyzed the data. M. Moreno and I. Vivaldo measured the structural  
307 properties and morphology of the materials. All of the authors contributed to the writing of this article.

308 **Acknowledgements:** The authors Maria de la Luz Mota and A. Carrillo want to thank to the program catedras-  
309 CONACYT. R. Ambrosio, J. Flores and R. Torrealba would like to acknowledge the VIEP-BUAP department for  
310 the support of the research.

311 **Conflicts of Interest:** “The authors declare no conflict of interest.”

## 312 References

- 313
- 314 1. Mathen, J.J.; Madhavan, J.; Thomas, A.; Edakkara, A.J.; Sebastian, J.; Joseph, G.P., Transparent ZnO-PVA  
315 binary composite for UV-A photo detector: optical, electrical and thermal properties followed by laser  
316 induced fluorescence, *J. Mater. Sci. Mater. Electron* 207, 28, 7190–7203. doi:10.1007/s10854-017-6400-1.
- 317 2. Wang, Z.; Han, N.M.; Wu, Y.; Liu, X.; Shen, X.; Zheng, Q.; Kim, J.K., Ultrahigh dielectric constant and low  
318 loss of highly-aligned graphene aerogel/poly(vinyl alcohol) composites with insulating barriers, *Carbon N.*  
319 *Y.* 2017, 123, 385–394. doi:10.1016/j.carbon.2017.07.079.
- 320 3. Dang, Z.-M.; Yuan, S.-J.-K.; Yao, H.; Liao, R.-J., Flexible Nanodielectric Materials with High Permittivity  
321 for Power Energy Storage, *Adv. Mater.* 2013, 25, 6334–6365. doi:10.1002/adma.201301752.
- 322 4. MacHado, W.S.; Hummelgen, I.A., Low-voltage poly(3-Hexylthiophene)/Poly(Vinyl Alcohol) field-effect  
323 transistor and inverter, *IEEE Trans. Electron Devices.* 2012, 59, 1529–1533. doi:10.1109/TED.2012.2187904.
- 324 5. Van Etten, E.A.; Ximenes, E.S.; Tarasconi, L.T.; Garcia, I.T.S.; Forte, M.M.C.; Boudinov, H., Insulating  
325 characteristics of polyvinyl alcohol for integrated electronics, *Thin Solid Films.* 2014, 568, 111–116.  
326 doi:10.1016/j.tsf.2014.07.051.
- 327 6. Mahendia, S.; Tomar, A.K.; Kumar, S., Electrical conductivity and dielectric spectroscopic studies of PVA-  
328 Ag nanocomposite films, *J. Alloys Compd.* 2010, 508, 406–411. doi:10.1016/j.jallcom.2010.08.075.
- 329 7. Son, D.I.; Park, D.H.; Choi, W.K.; Cho, S.H.; Kim, W.T.; Kim, T.W., Carrier transport in flexible organic  
330 bistable devices of ZnO nanoparticles embedded in an insulating poly(methyl methacrylate) polymer layer,  
331 *Nanotechnology.* 2009, 20, 0–6. doi:10.1088/0957-4484/20/19/195203.
- 332 8. Kazemi, A.S.; Afzalzadeh, R.; Abadyan, M., ZnO Nanoparticles as Ethanol Gas Sensors and the Effective  
333 Parameters on Their Performance, *J. Mater. Sci. Technol.* 2013, 29, 393–400. doi:10.1016/j.jmst.2013.03.009.
- 334 9. Wu, W.; Huang, X.; Li, S.; Jiang, P.; Toshikatsu, T., Novel three-dimensional zinc oxide superstructures for  
335 high dielectric constant polymer composites capable of withstanding high electric field, *J. Phys. Chem. C.*  
336 2012, 116, 24887–24895. doi:10.1021/jp3088644.
- 337 10. Devi, P.I.; Ramachandran, K., Dielectric studies on hybridised PVDF-ZNO nanocomposites, *J. Exp. Nanosci.*  
338 2011, 6, 281–293. doi:10.1080/17458080.2010.497947.
- 339 11. Sugumaran, S.; Bellan, C.S.; Muthu, D.; Raja, S.; Bheeman, D.; Rajamani, R., Novel hybrid PVA-InZnO  
340 transparent thin films and sandwich capacitor structure by dip coating method: preparation and  
341 characterizations, *RSC Adv.* 2015, 5, 10599–10610. doi:10.1039/C4RA14817G.

- 342 12. Hdidar, M.; Chouikhi, S.; Fattoum, A.; Arous, M.; Kallel, A., Influence of TiO<sub>2</sub>rutile doping on the  
343 thermal and dielectric properties of nanocomposite films based PVA, *J. Alloys Compd.* 2018, 750, 375–383.  
344 doi:10.1016/j.jallcom.2018.03.272.
- 345 13. Komarov, S.A.; Komarov, A.S.; Barber, D.G.; Lemes, M.J.L.; Rysgaard, S., Open-Ended Coaxial Probe  
346 Technique for Dielectric Spectroscopy of Artificially Grown Sea Ice, *IEEE Trans. Geosci. Remote Sens.* 2016,  
347 54, 4941–4951. doi:10.1109/TGRS.2016.2553110.
- 348 14. Roy, A.S.; Gupta, S.; Sindhu, S.; Parveen, A.; Ramamurthy, P.C., Dielectric properties of novel PVA/ZnO  
349 hybrid nanocomposite films, *Compos. Part B Eng.* 2013, 47, 314–319. doi:10.1016/j.compositesb.2012.10.029.
- 350 15. Karthikeyan, B.; Pandiyarajan, T.; Mangalaraja, R. V., Enhanced blue light emission in transparent  
351 ZnO:PVA nanocomposite free standing polymer films, *Spectrochim. Acta - Part A Mol. Biomol. Spectrosc.*  
352 2016, 152, 485–490. doi:10.1016/j.saa.2015.07.053.
- 353 16. Rashmi, S.H.; Raizada, A.; Madhu, G.M.; Kittur, A.A.; Suresh, R.; Sudhina, H.K., Influence of zinc oxide  
354 nanoparticles on structural and electrical properties of polyvinyl alcohol films, *Plast. Rubber Compos.* 2015,  
355 44, 33–39. doi:10.1179/1743289814Y.0000000115.
- 356 17. Schroeder, R.; Majewski, L.A.; Grell, M., High-performance organic transistors using solution-processed  
357 nanoparticle-filled high-k polymer gate insulators, *Adv. Mater.* 2005, 17, 1535–1539.  
358 doi:10.1002/adma.200401398.
- 359 18. Bouropoulos, N.; Psarras, G.C., Moustakas, N.; Chrissanthopoulos, A.; Baskoutas, S., Optical and dielectric  
360 properties of ZnO-PVA nanocomposites, *Phys. Status Solidi Appl. Mater. Sci.* 2008, 205, 2033–2037.  
361 doi:10.1002/pssa.200778863.
- 362 19. Yeow, Y.K.; Abbas, Z.; Khalid, K.; Rahman, M.Z.A., Improved dielectric model for polyvinyl alcohol-water  
363 hydrogel at microwave frequencies, *Am. J. Appl. Sci.*, 2010, 7, 270–276. doi:10.3844/ajassp.2010.270.276.
- 364 20. Latif, I.; AL-Abodi, E. E.; Badri, D. H.; Al Khafagi, J., Preparation, Characterization and Electrical Study of  
365 (Carboxymethylated Polyvinyl Alcohol/ZnO) Nanocomposites, *Am. J. Polym. Sci.* 2013, 2, 135–140.  
366 doi:10.5923/j.ajps.20120206.01.
- 367 21. Chandrakala, H.N.; Ramaraj, B.; Shivakumaraiah; Madhu, G.M., The influence of zinc oxide-cerium oxide  
368 nanoparticles on the structural characteristics and electrical properties of polyvinyl alcohol films, *J. Mater.*  
369 *Sci.* 2012, 47, 8076–8084. doi:10.1007/s10853-012-6701-y.
- 370 22. Levinson, L.M.; Philipp, H.R., Low-temperature ac properties of metal-oxide varistors, *J. Appl. Phys.* 1978,  
371 49, 6142–6146. doi:10.1063/1.324536.
- 372 23. Wang, G.; Deng, Y.; Xiang, Y.; Guo, L., Fabrication of radial ZnO nanowire clusters and radial ZnO/PVDF  
373 composites with enhanced dielectric properties, *Adv. Funct. Mater.* 2008, 18, 2584–2592.  
374 doi:10.1002/adfm.200800109.
- 375 24. Roscow, J.I.; Bowen, C.R.; Almond, D.P., Breakdown in the Case for Materials with Giant Permittivity?,  
376 *ACS Energy Lett.* 2017, 2, 2264–2269. doi:10.1021/acseenergylett.7b00798.
- 377 25. Nan, C.W.; Shen, Y.; Ma, J., Physical Properties of Composites Near Percolation, *Annu. Rev. Mater. Res.*  
378 2010, 40, 131–151. doi:10.1146/annurev-matsci-070909-104529.
- 379 26. Chen, X.; Liang, F.; Lu, W.; Jin, Z.; Zhao, Y.; Fu, M. High Permittivity Nanocomposites Embedded with  
380 Ag/TiO<sub>2</sub> Core-Shell Nanoparticles Modified by Phosphonic Acid, *Polymers* 2018, 10, 586.  
381 doi:10.3390/polym10060586.